Open Access

Male Infertility

ORIGINAL ARTICLE

Mkrn2 deficiency induces teratozoospermia and male infertility through p53/PERP-mediated apoptosis in testis

Ying-Chen Qian[1],*, Yun-Xia Xie[1],*, Chao-Shan Wang[1], Zhu-Mei Shi[2], Cheng-Fei Jiang[1], Yun-Yi Tang[1], Xu Qian[1], Lin Wang[3], Bing-Hua Jiang[1,3,4]

The apoptosis that occurs in the immature testis under physiological conditions is necessary for male germ cell development, whereas improper activation of apoptosis can impair spermatogenesis and cause defects in reproduction. We previously demonstrated that in mice, the makorin-2 (*Mkrn*2) gene is expressed exclusively in the testis and its deletion leads to male infertility. To understand the potential molecular mechanism, in this study, we found that levels of apoptosis in the testis were abnormally high in the absence of *Mkrn*2. To identify specific gene(s) involved, we performed digital gene expression profiling (DGE) and pathway analysis via gene set enrichment analysis (GSEA) and the Kyoto Encyclopedia of Genes and Genomes (KEGG) database, and we found that MKRN2 inhibits p53 apoptosis effector related to PMP22 (PERP) expression and that levels of the protein in sperm samples have an inverse correlation with infertility levels. GSEA additionally indicated that PERP is a negative regulator of spermatogenesis and that its ectopic expression induces male infertility. Further, Gene Expression Omnibus (GEO) dataset analysis showed that p53, upstream of PERP, was upregulated in oligoasthenoteratozoospermia (OAT). These observations suggest that *Mkrn*2 is crucial for protecting germ cells from excessive apoptosis and implicate *Mkrn*2-based suppression of the p53/PERP signaling pathway in spermatogenesis and male fertility.

INTRODUCTION

Spermatogenesis is a complex and elaborated process, whereby spermatogonia proliferate and differentiate into spermatozoa. Notably, during this process, approximately 75% of all progeny of spermatogonia is destroyed by germ cell apoptosis.[1,2] Previous studies demonstrated that the dysregulation of germ cell apoptosis may cause suboptimal male reproductive function and even male infertility.[3,4] Apoptosis in the testis can be induced by factors that disrupt spermatogenesis. For example, fenvalerate induces germ cell apoptosis in the testis by acting on the Fas/FasL signaling pathway.[5] Pulsed or continuous electromagnetic field induces apoptosis of the spermatogenic cells in mouse through p53/p21-mediated apoptotic signaling pathway and thus results in male fertility.[6] Similarly, decrease of p53 levels affects germ cell homeostasis during spermatogenesis.[7] Deficiency of the *Magea* gene cluster leads to small testes and high rates of apoptosis during the first wave of spermatogenesis, but the *Magea* gene cluster regulates male germ cell apoptosis without affecting the fertility in mice.[8] Recently, exposure to environmental pollutants has also been suggested to cause male reproductive defects.[9,10] Furthermore, the treatments of radiation and chemotherapeutic drugs in current cancer also cause germ cell

apoptosis and increase the risk of male infertility.[11,12] Thus, there is an urgent need to understand the mechanisms that underlie excessive apoptosis in spermatogenic cells, as well as to identify ways to prevent this phenomenon. The makorin (*MKRN*) gene family encodes putative ribonucleoproteins that have a distinctive array of zinc finger domains.[13] Makorin-2 (*MKRN*2), which was first identified in the human CD34+ hematopoietic stem/progenitor cells, was only recently added to the Makorin family.[14] This zinc finger protein contains the typical C3HC4 protein–protein interaction motif (termed the RING domain) that is common to many proteins expressed in various tissues and cell lines.[15,16] We previously demonstrated that in mice, its mRNA and protein are expressed most prominently in the testis and at low levels in various other tissues.[17] Immunohistochemical analysis revealed that MKRN2 protein is located mainly in the Sertoli cells and spermatids, suggesting that it plays an important role in spermiogenesis and spermiation. Furthermore, we generated *Mkrn*2-knockout (KO) mice and found that KO mice were infertile; no pups were born during a 4-month period of mating. Moreover, spermatozoa were in low number, with poor motility and abnormal morphology in *Mkrn*2-KO mice. However, further studies are required to fully understand the molecular mechanisms

[1]Department of Pathology, Nanjing Medical University, Nanjing 210029, China; [2]Department of Neurosurgery, The First Affiliated Hospital of Nanjing Medical University, Nanjing 210029, China; [3]The Academy of Medical Sciences, Zhengzhou University, Zhengzhou 450001, China; [4]Department of Pathology, The University of Iowa, Iowa City, IA 52242, USA.
*These authors contributed equally to this work.
Correspondence: Dr. BH Jiang (binghjiang@yahoo.com)

responsible for the sterility caused by *Mkrn*2 deficiency in mammals.

Here, we identified differential expression genes in *Mkrn*2-KO and *Mkrn*2 wide-type (WT) mice and further found an increase in apoptosis of the testis in the absence of *Mkrn*2. In particular, we found the p53 signaling pathway to be highly upregulated, which is known to be related to apoptosis,[18–20] implying that apoptosis could play a major role in the infertility associated with the *Mkrn*2 KO. In this study, we further showed that MKRN2 inhibits p53/PERP signaling, protecting germ cells from excessive apoptosis.

MATERIALS AND METHODS

Mkrn2-KO mice
*Mkrn*2-heterozygous and *Mkrn*2-KO mice were generated as previously described,[17] and the genotype of their pups was determined by polymerase chain reaction (PCR). The tail DNA in mice was extracted and mutant *Mkrn*2 allele was identified by PCR as described[17] (**Supplementary Table 1**). All mice were housed and maintained under specific pathogen-free conditions, and all animal experiments were approved by the Committee of Laboratory Animal Experimentation of Nanjing Medical University (Nanjing, China). All methods were performed in accordance with the relevant guidelines and regulations.

Cell culture
*Mkrn*2-WT and *Mkrn*2-KO primary mouse embryonic fibroblasts (MEFs) were derived from 13.5-day embryos and cultured as described,[17] and 293T cells were cultured in Dulbecco's modified Eagle's medium (DMEM, catalog# 10566016, Gibco, Carlsbad, CA, USA) supplemented with 10% (*v/v*) fetal bovine serum (FBS, catalog# 100500, Gemini, West Sacramento, CA, USA), 100 U ml^{-1} penicillin, and 100 µg ml^{-1} streptomycin (1% [*w/v*] PS, catalog# 15070063, Gibco) and were maintained at 37°C and at 5% (*v/v*) CO_2.

Construction of expression vector and transfection
The Mkrn2-mus expression vector and its control vector (pCMV-C-Flag) were acquired as described.[17] The p53 expression vector (pHMT.wt p53) was a gift from James Sherley (catalog# 12139, Addgene plasmid, Boston, MA, USA). The pGIPZ-Mkrn2-ShRNA vector and control negative vector (pGIPZ) were acquired as described.[17] Lipofectamine 2000 reagent (Invitrogen, Carlsbad, CA, USA) was used to transfect the plasmids or negative control vector, shRNA or negative control shRNA into MEFs and 293T cells following the manufacturer's protocol.

Immunohistochemical analysis
Testes were obtained from 12-day-old mice, dissected, and immersed in Bouin's fixatives for 24 h before being embedded in paraffin. Sections (4 µm) were stained with hematoxylin and eosin (H and E) for histological examination. For further immunohistochemical analysis, the sections were deparaffinized in xylene and hydrated in a graded ethanol series. The peroxidase in the section tissues was eliminated using 3% (*v/v*) hydrogen peroxide at room temperature for 20 min, and then, sections were treated for antigen recovery with 0.01 mol l^{-1} sodium citrate solutions. The sections were blocked with 1% Bovine Serum Albumin (BSA) for 1 h at room temperature before incubation primary antibody at 4°C overnight. For immunohistochemical analysis, anti-MKRN2 antibody (catalog# NB100-55250, Novus Biologicals, Inc., Littleton, CO, UK) was used at a 1:2000 dilution, anti-cleaved caspase 3 antibody (catalog# 19677-1-AP, Proteintech, Wuhan, China) was used at a 1:200 dilution, anti-BCL2 Associated X (BAX) antibody (catalog# 50599-2-Ig, Proteintech) was used at a 1:100 dilution, anti-p53 apoptosis effector related to PMP22 (PERP) antibody (catalog# AB_48032,

Abcam, Inc., London, UK) was used at a 1:100 dilution, and anti-p53 (DO-7) antibody (catalog# 48818, CST, Inc., Boston, MA, USA) was used at a 1:100 dilution. After the samples were incubated with secondary antibody, signals were detected using the diaminobenzidine (DAB) Histochemistry Kit (catalog# TL-015-HD, Invitrogen, Boston, MA, USA). The relative integrated option density (IOD) values of each section were analyzed by Image-Pro Plus software (Media Cybernetics, Bethesda, MD, USA).

Immunoblot
Tissues ground in liquid nitrogen were lysed on ice for 30 min in ice-cold Radio-Immunoprecipitation Assay (RIPA) buffer (catalog# P0013C, Beyotime Biotechnology, Shanghai, China) supplemented with protease inhibitor cocktail (catalog# P8340-1 ml, Sigma, San Francisco, CA, USA). The cells lysates were centrifuged at 21 100 *g* at 4°C for 15 min. The tissues lysates were subjected to three sets of 15-s pulses between pulses for 15 min on ice and then centrifuged at 21 100 *g* at 4°C for 1 h. The extracts were subjected to immunoblot using antibodies for MKRN2 (1:2000 dilution; catalog# NB100-55250, Novus Biologicals), PERP (1:500 dilution; catalog# AB_48032, Abcam), p53 (DO-7) (1:1000 dilution; catalog# 48818, CST), and anti-p53 (acetyl-K120) (1:1000 dilution; catalog# HW-186, SAB, Inc., Nanjing, China) as described above. In addition, the housekeeping protein β-actin antibody (1:2500 dilution; catalog# 60008-1-Ig, Proteintech) was used as a loading control. The integrated density values were used to calculate the gray values by Image J software (National Institutes of Health, Bethesda, MD, USA).

RNA extraction, reverse transcription-polymerase chain reaction (RT-PCR), and quantitative real-time PCR (qRT-PCR) analysis
Total RNAs were extracted from *Mkrn*2-WT and *Mkrn*2-KO MEFs, as well as from 293T cells, and purified using TRIzol reagent (catalog# 15596018, Invitrogen) according to the manufacturer's instructions. RT-PCR was performed using the HiScript II Q RT SuperMix (+gDNA wiper) (catalog# R323, Vazyme Biotech, Nanjing, China). qRT-PCR was performed using ChamQ SYBR Color qPCR Master Mix (High ROX Premixed) (catalog# Q441, Vazyme Biotech Co., ltd.) on a 7900HT system. *Gapdh*, *β-actin*, and *Hprt* levels were used as internal controls,[21,22] and relative quantification (2$^{-\Delta\Delta Ct}$) was used to calculate fold changes. The primer sequences are listed in **Supplementary Table 2**.

Digital gene expression profiling and KEGG-based pathway analysis
Total RNAs extracted from the *Mkrn*2-WT and *Mkrn*2-KO MEFs were sequenced by Illumina HiSeq™ 2000 sequencing system. Mouse reference genome used was mm9 and alignment software used was STAR. The counts were obtained by htseq-count, and transcripts per million (TPM) values were calculated. Pathway analysis of the datasets was performed using the Kyoto Encyclopedia of Genes and Genomes (KEGG) and ggplot2. In the Volcano plot, the threshold for differential expression genes is log fold change (FC) >1 or <−1 ($P < 0.05$).

Gene set enrichment analysis (GSEA)
The samples in Gene Expression Omnibus (GEO) dataset GSE6872, which contains sperm sample microarray data, were split into two groups on the basis of expression levels of PERP. The GSEA program was employed to analyze the spermatogenesis signal enrichment scores in the PERP-high versus PERP-low expression groups from the Molecular Signatures Database (MSigDB) gene set (Gene Ontology (GO) male gamete generation; HALLMARK: SPERMATOGENESIS).

TUNEL assay

The terminal deoxynucleotidyl transferase dUTP nick end labeling (TUNEL) assay was performed with Click-iT™ TUNEL Colorimetric IHC Detection Kit (catalog# C10625, Invitrogen, Boston, MA, USA) according to the manufacturer's instructions. Briefly, the fixed and permeabilized tissues[23] were incubated with 1 U of DNase I (catalog# 18068015, Invitrogen, Boston, MA, USA) diluted in 1× DNase I reaction buffer (20 mmol l^{-1} Tris-HCl, pH 8.4, 2 mmol l^{-1} MgCl$_2$, 50 mmol l^{-1} KCl) for 30 min at room temperature. Afterward, the samples were washed once with deionized water and then reacted with the terminal deoxynucleotidyl transferase (TDT) enzyme. Finally, 1× DAB reaction mixture was added to each sample, and the reactions proceeded at room temperature for 5 min.

Gene signature analysis

PERP signatures were analyzed using the spermatogenesis signal enrichment scores. The p53 signature were analyzed using the GEO dataset GSE6872.[24,25] The *MKRN*2 signatures were analyzed using the HALLMARK SPERMATOGENESIS gene set described above for the GSE6872 dataset (https://www.ncbi.nlm.nih.gov/geo/query/acc.cgi?acc=GSE6872).[24,25]

Statistical analyses

Data are presented as the means ± standard deviation (s.d.). Statistical analysis and Spearman's correlation analysis were performed using GraphPad Prism 7 (GraphPad Software, San Diego, CA, USA). The two-way ANOVA with Bonferroni *post hoc* test was used to evaluate the differences between the multiple groups using GraphPad Prism 7. The two-tailed Student's *t*-test was used to analyze the quantitative variables between the two groups, assuming equal or unequal variance determined by the *F*-test of equality of variances. Student's *t*-test was carried out with SPSS version 22.0 (SPSS Inc., Chicago, IL, USA). Correlations between the *MKRN*2 and *PERP* expression signatures were analyzed by Pearson's correlation analysis. The differences were considered statistically significant at *P* < 0.05.

RESULTS

The sets of differential expression genes (DEGs) enriched in Mkrn2 KO were compared to those from WT mice

To identify the mechanism responsible for the *Mkrn*2-KO phenotype, we extracted RNAs from MEFs of *Mkrn*2-KO and *Mkrn*2-WT embryos and profiled gene expression levels by DGE. Analysis of the raw data revealed many DEGs existing in the *Mkrn*2-KO versus *Mkrn*2-WT samples (**Figure 1a** and **1b**), among which 614 genes were upregulated (red) and 754 were downregulated (blue). To identify the genes most likely to be responsible for the *Mkrn*2-KO phenotype, we performed KEGG analysis using the DEGs. The results showed that these gene sets were enriched for multiple pathways in the context of the *Mkrn*2 deficiency (**Figure 1c**). Furthermore, using the online KEGG pathway maps website (https://www.genome.jp/kegg/tool/map_pathway2.html), we found that there were several crucial mediators of the p53 pathway in DEGs (Bbc3, Bax, Perp, Apaf1, Atr, Cdk1, Chek1, Ccng2, Cytc, Igf1, Igfbp3, Pmaip1, Sesn1, and Sesn2).
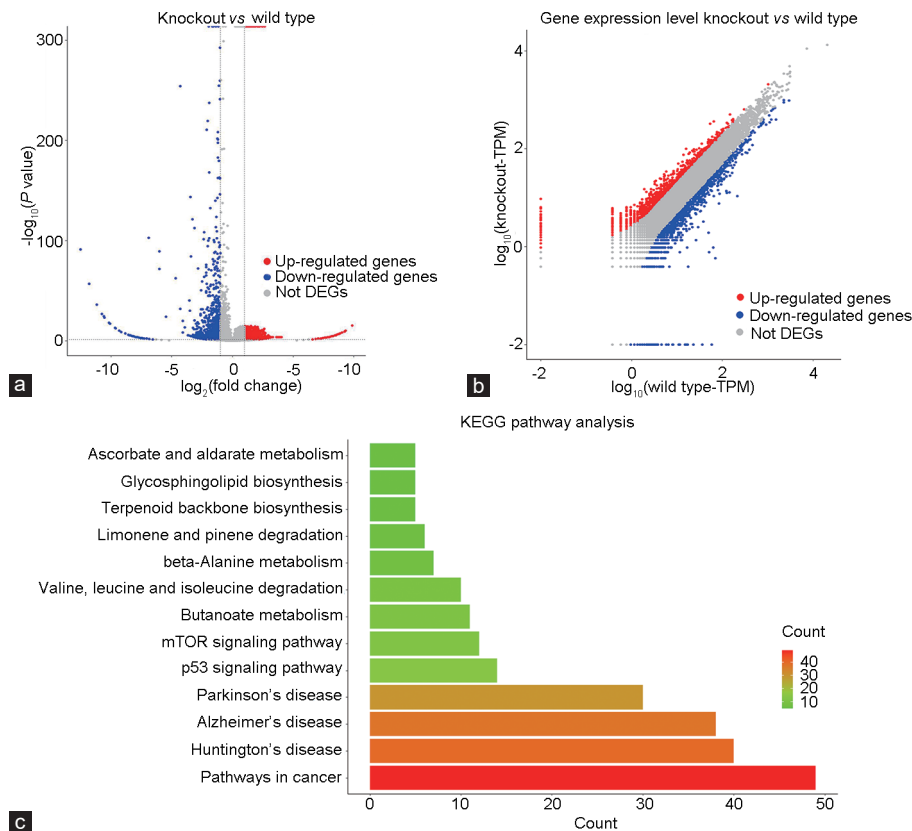

Figure 1: The sets of DEGs enriched in *Mkrn*2-KO were compared to those from the *Mkrn*2-WT mice. (**a**) Volcano plot of DEGs in MEFs isolated from *Mkrn*2-KO and *Mkrn*2-WT mice. DEGs are color coded according to whether they are up- or down-regulated (logFC >1 or <−1, *P* < 0.05); 614 genes upregulated in *Mkrn*2-KO group, red; 754 genes downregulated in *Mkrn*2-KO group, blue. (**b**) Scatter plot illustrating relative gene expression levels by group, with color coding as in **a**. (**c**) Biological pathways represented among the identified DEGs, as determined by KEGG analysis. DEG: differential expression gene; *Mkrn*2: makorin-2; KO: knockout; WT: wild type; MEF: mouse embryonic fibroblast; KEGG: Kyoto Encyclopedia of Genes and Genomes; logFC: log fold change; mTOR: Mechanistic Target Of Rapamycin Kinase.

MKRN2 inhibited expression of PERP, apoptosis modulator

To understand the effects of MKRN2 on p53 pathway signaling better, we first assessed the levels of identified DEGs that are part of the p53 pathway by qRT-PCR. This analysis revealed that the levels of most of the DEGs were changed, with the expression levels of *PERP* mostly affected (**Figure 2a** and **Supplementary Figure 1**). Second, we tested the effects of MKRN2 overexpression and knockdown on PERP expression levels in 293T cells, which express MKRN2 at low levels under normally physiological conditions. Analysis by qRT-PCR confirmed that *Perp* levels were lower in the presence of the *Mkrn*2 expression vector than in its absence (gray *vs* blue) (**Figure 2b**). Moreover, it showed that the effect was specific to MKRN2 because co-transfection with an Mkrn2-targeting shRNA vector counteracted the effect of MKRN2 expression (red). Western blot confirmed these findings at the protein levels (**Figure 2c** and **Supplementary Figure 2a**). Third, we investigated the correlation between *MKRN*2 and *PERP* expression levels in the human samples in the GEO dataset GSE6872 (sperm samples for sperm specimens from 8 patients with oligoasthenoteratozoospermia [OAT] and 13 normal subjects). We found an inverse correlation between levels of *MKRN*2 and *PERP* ($r = -0.7376$, $P = 0.0001$; **Figure 2d**).

PERP levels were negatively correlated with spermatogenesis

PERP expression levels were higher in sperm samples from the OAT patients than the normal subjects (**Figure 3a**). Furthermore, GSEA results of *PERP*-high and *PERP*-low expression groups of the GSE6872 dataset indicated that the male gamete generation and spermatogenesis gene sets were enriched for *PERP*-low expression groups, showing that high *PERP* expression is detrimental to spermatogenesis (**Figure 3b** and **3c**). Spearman's correlation analysis also showed an inverse rank correlation between *PERP* expression levels and spermatogenesis in the sperm expression dataset ($r = -0.6208$, $P = 0.0027$; **Figure 3d**).

Mkrn2-KO induced PERP expression mediated by p53

To determine whether the p53 family members participate in the MKRN2/PERP pathway, we assayed the expression level of p53 using the GSE6872 dataset. The results confirmed that p53 levels were elevated, which is consistent with upregulation of *PERP*, in the sperm samples from the OAT patients versus normal subjects (**Figure 4a**). We analyzed the correlation between MKRN2 and p53/PERP in MEFs. Western blot demonstrated that the expression levels of p53 and PERP were upregulated in *Mkrn*2-KO MEFs (**Figure 4b** and **Supplementary Figure 2b**). In *Mkrn*2-KO MEFs, overexpression of p53 reversed the inhibition of PERP expression in the presence of the MKRN2 expression (**Figure 4c** and **Supplementary Figure 2c**). We evaluated the expression levels of PERP in 293T cells by transfecting with vector and negative control vector (CON), Mkrn2 and CON, and Mkrn2 and p53. We found that the expression changes of PERP were consistent with the above results as in MEFs (**Figure 4d** and **Supplementary Figure 2d**).

p53/PERP levels were upregulated in Mkrn2-KO mouse testes

We used TUNEL assay and immunohistochemistry (IHC) for detecting the levels of cleaved caspase 3 and BAX to determine if *Mkrn*2-KO mice had higher levels of testicular apoptosis than the *Mkrn*2 WT (**Figure 5a** and **Supplementary Figure 3a–3d**). Histological analysis revealed higher levels of p53 and PERP expression in the testes of *Mkrn*2-KO than *Mkrn*2-WT mice (**Figure 5b** and **5c**, and **Supplementary Figure 3a**), and these results are consistent with Western blot for p53 and PERP in *Mkrn*2 KO compared to WT testis (**Figure 5d** and **Supplementary Figure 2e**).

DISCUSSION

Mammalian spermatogenesis is controlled by many factors, among which the regulation of gene expression during this period is pivotal.[26,27] However, the mechanisms underlying the expression levels of spermatogenesis-related genes remain largely unknown.
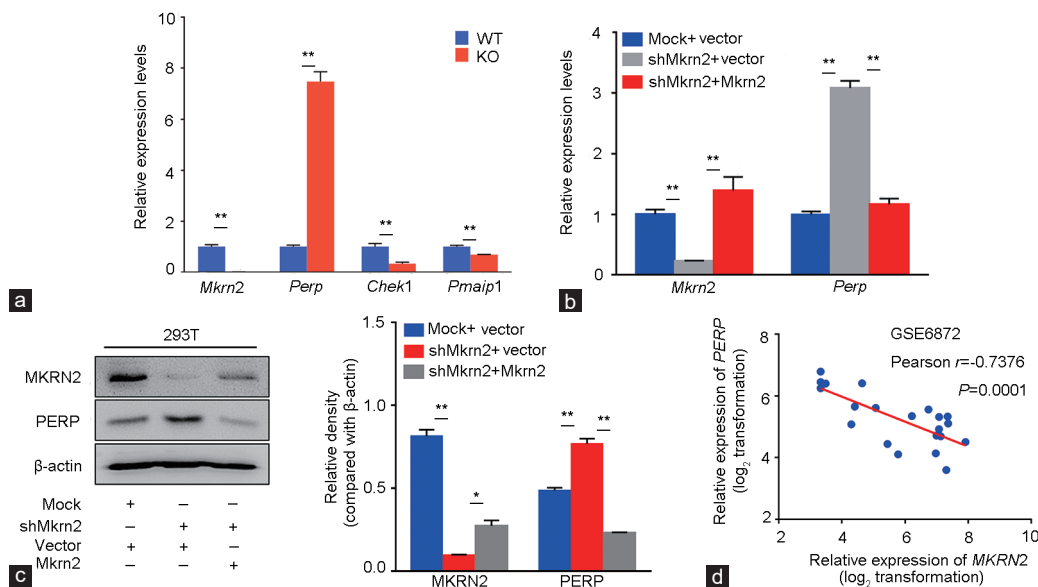
Figure 2: DEGs and PERP expression levels in *Mkrn*2-KO cells and tissues. (**a**) Expression levels of DEGs for the *Mkrn*2-KO and *Mkrn*2-WT MEFs are analyzed by qRT-PCR. Data are presented and analyzed by the Student's *t*-test from three independent experiments performed in triplicate. **Significant difference compared with WT group ($P < 0.01$). 293T cells were co-transfected with an Mkrn2 shRNA (shMkrn2) or negative control (Mock) vector plus an MKRN2 expression vector or control vector. (**b**) qRT-PCR is used to analyze the mRNA expression of *PERP*. Data are presented as mean ± s.d. from three independent experiments performed in triplicate. (**c**) Western blot is used to analyze the protein expression of PERP, densitometric analysis of Western blot signals (right). (**b** and **c**) Results are presented and analyzed by the two-way ANOVA, *Significant difference at $P < 0.05$, **Significant difference at $P < 0.01$. (**d**) Correlation between *MKRN*2 and *PERP* expression levels in GEO dataset GSE6872 (contains sperm samples), as analyzed by Pearson's correlation analysis. DEG: differential expression gene; *Mkrn*2: makorin-2; KO: knockout; WT: wild type; PERP: p53 apoptosis effector related to peripheral myelin protein 22 (PMP22); qRT-PCR: quantitative real-time polymerase chain reaction; s.d.: standard deviation; MEF: mouse embryonic fibroblast; GEO: Gene Expression Omnibus.
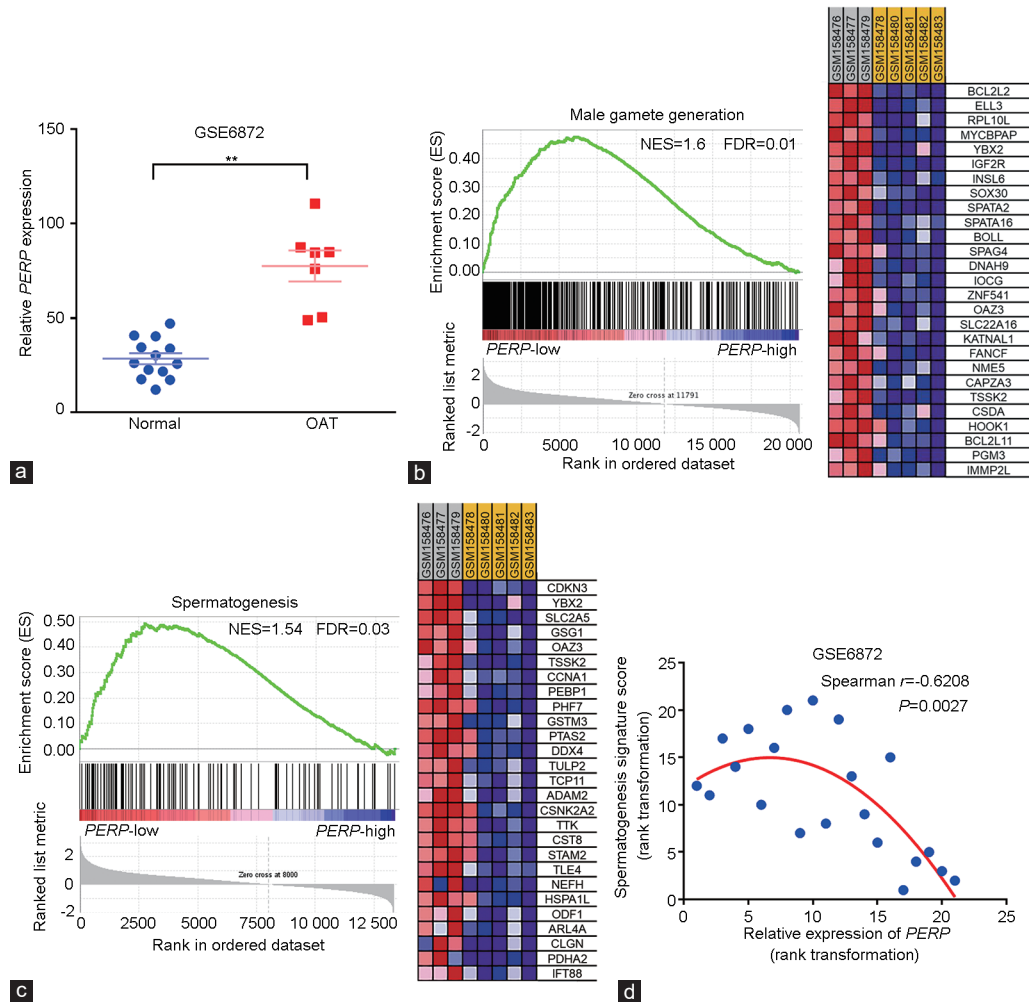
Figure 3: Correlation of PERP levels with spermatogenesis. (**a**) Relative expression levels of the *Mkrn*2 in normal and OAT sperm samples from the GSE6872 dataset. Data are presented and analyzed by two-tailed, unpaired Student's *t*-test. **Significant differences compared with WT group ($P < 0.01$). (**b**) Enrichment and ranking of genes in the *PERP*-high and *PERP*-low expression groups of the GSE6872 dataset are assessed by GSEA analysis (C5: GO gene sets; BP: GO biological process; gene set: male gamete generation) and the corresponding clustering heatmap of genes that contribute most to enrichment score is on the right. (**c**) Enrichment and ranking of genes in the *PERP*-high and *PERP*-low expression groups of the GSE6872 dataset are assessed by GSEA analysis (H: hallmark gene set; gene set: spermatogenesis) and the corresponding clustering heatmap of genes that contribute most to enrichment score is on the right (*PERP*-low datasets: GSM158476, GSE158477, and GSM158479 and *PERP*-high datasets: GSM158478, GSM158480, GSM158481, GSM158482, and GSM158483). (**d**) Correlations between spermatogenic signature scores and *PERP* expression levels are determined by Spearman's rank correlation analysis. Mkrn2: makorin-2; KO: knockout; WT: wild type; PERP: p53 apoptosis effector related to PMP22; GSEA: gene set enrichment analysis; OAT: oligoasthenoteratozoospermia.

MKRN2, a member of the MKRN protein family, was predicted to function as an ubiquitin E3 ligase.[28] Early studies reported that it is expressed in all cells of hematopoietic origin,[29] with particularly high expression in immune cells, where it promotes the ubiquitination and degradation of p65.[28] In our previous study, we generated a novel mouse model in which exons 2–6 of the *Mkrn*2 gene cluster were deleted and exons 7 and 8 contained frameshift mutations.[17] This gene KO resulted in an obvious reduction in testis size and disruption of ectoplasmic specialization (ES), leading to abnormalities in the sperm head and failure of spermiation.[30,31] These defects in *Mkrn*2 also suppressed expression of outer dense fiber protein 2 (Odf2) in germ cells, disrupting the flagellar assembly of sperm tails. However, the mechanism and function of the MKRN2 protein during the male germ cell development and spermatogenesis remain largely understudied.

Several studies of spermatogenesis have shown that both spontaneous and stress-induced apoptosis play key roles in maintaining the homeostasis of different cell types and eliminating germ cells that are defective or carry mutations.[32–34] Those studies showed that germ cell apoptosis occurs not only during the fetal period but also before puberty and during adult stages.[35,36] Additional studies have also shown that the dysregulation of germ cell apoptosis may cause suboptimal male reproductive function and even male infertility.[37,38] To maintain the ratio between Sertoli cells and maturing germ cells, the first wave of apoptosis is required for germ cell development.[39] In this process, in mice at postnatal 10 days (P10), germ cells enter meiotic prophase; subsequently at P12, spermatocytes start to their transition to spermatids. Our study showed that the deletion of *Mkrn*2 disrupts the balance between germ cells survival and apoptosis, which leads to spermatogenic dysfunction in mice.

To explore *Mkrn*2 function in spermatogenesis, we used DGE and bioinformatic techniques to identify the DEGs in the *Mkrn*2-KO and *Mkrn*2-WT mice. We found differential expressions of 1368 such genes
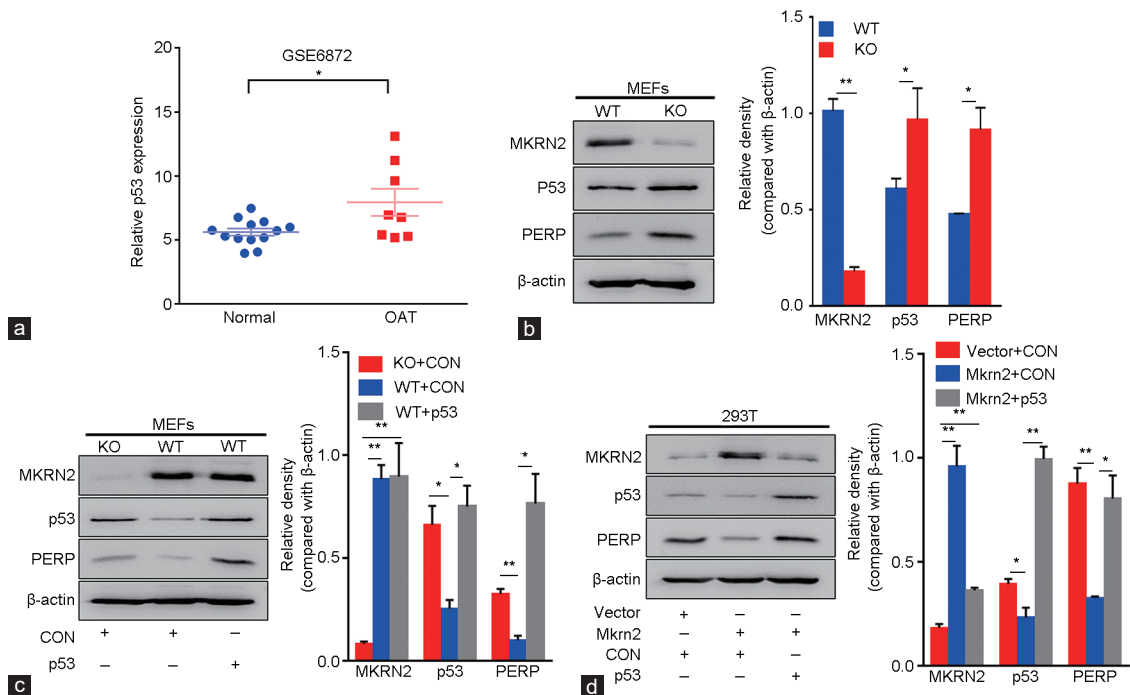
Figure 4: Association of PERP and p53 expression levels in *Mkrn*2-KO cells and tissues. (**a**) Expression levels of p53 are analyzed by GEO dataset GSE6872. Data are presented and analyzed by two-tailed, unpaired Student's *t*-test. *Significant difference compared with the normal group ($P < 0.05$). (**b**) Expression levels of MKRN2, p53, and PERP in MEFs are analyzed by Western blot (left), densitometric analysis of Western blot signals (right). (**c**) Expression levels of p53 and PERP in MEFs transfected with a p53 vector or CON as indicated are analyzed by Western blot (left), densitometric analysis of Western blot signals (right). (**d**) PERP expression levels are determined by Western blot in 293T cells co-transfected with vector and control, Mkrn2 and CON, Mkrn2 and p53, respectively (left), densitometric analysis of Western blot signals (right). (**c** and **d**) Results are presented and analyzed by the two-way ANOVA from three independent experiments and each performed for three times. *Significant difference at $P < 0.05$, **Significant difference at $P < 0.01$. CON: negative control vector; Mkrn2: makorin-2; KO: knockout; WT: wild type; PERP: p53 apoptosis effector related to PMP22; GEO: Gene Expression Omnibus; MEF: mouse embryonic fibroblast.

($P < 0.05$). Furthermore, the p53-signaling pathway was found to be mostly deregulated from analysis of the online KEGG pathway maps database because its activation could easily lead to excessive apoptosis of the mutant spermatocytes.[40] The expression levels of the DEGs of the p53 signal pathway in MEFs isolated from *Mkrn*2-KO and *Mkrn*2-WT mice by qRT-PCR confirmed that *Perp* levels were greatly increased in the former cells, which have important roles in the regulation of apoptosis in cancer.[41–43] Interestingly, our analysis with the GSE6872 dataset revealed that the expression of *PERP* was not only negatively correlated with *MKRN*2 expression but also was negatively correlated to the extent of spermatogenesis. Previous study has provided evidence that p53 has an effect on spermatogenesis including the role for meiotic checkpoint control and germ cell quality. Consistently, our Western blotting result showed that p53 expression and MKRN2 levels have a negative correlation and that while p53 was overexpressed, PERP expression can be increased. Our results showed that p53/PERP is an important downstream of *Mkrn*2 during spermiogenesis and spermiation. It was reported that the expression of PERP stabilized active p53 via modulation of p53-mouse double-minute 2 protein (MDM2) interaction and positively influenced the transcription level of MDM2 depending on p53.[44] To determine whether *Mkrn*2 KO affects protein levels of p53 and PERP as well as the expression of MDM2, we detected MDM2 expression levels in *Mkrn*2-WT and *Mkrn*2-KO MEFs, and the results showed no significant difference of MDM2 levels between *Mkrn*2-WT and *Mkrn*2-KO MEFs (results are not shown). Meanwhile, *Mdm*2 is also not existed in DEGs analysis. It was suggested that cellular heterogeneity increased the

complexity of modeling gene regulation.[45] In our model, we suggest that the absence of *Mkrn*2 may affect other molecules for regulating MDM2, which may cause the difference. However, the influence of *Mkrn*2 on the expression levels of MDM2 would be interesting to be further explored in the future. Recent studies have indicated that the modification of p53 may be involved in its biological regulation,[46] including by acetylation which may increase p53 activity.[47] More importantly, acetylated p53 (K120) plays a crucial role in the process of p53-mediated apoptosis.[48,49] To investigate the correlation between *Mkrn*2 and acetyl-p53, we analyzed the levels of the acetyl-p53 (K120) protein and showed that *Mkrn*2 KO upregulated the expression levels of acetyl-p53 (K120) (**Supplementary Figure 4**). This result suggests that the *Mkrn*2-inducing p53/PERP apoptosis pathway may be regulated through the acetylation of p53 (K120). However, whether *Mkrn*2 KO activates the p53-induced apoptosis pathway primarily through the abnormal modification and acetylation of p53 needs to be further investigated. Taken together, these results indicate that *Mkrn*2 KO may regulate the first wave of apoptosis to affect the germ cell development through p53 apoptosis pathway.

Our study provides the first molecular insight into the function of the *Mkrn*2 gene in the testicular development, including roles in the maintenance of normal testis size and protection of germ cells from excessive apoptosis. Furthermore, our results demonstrate that a lack of *Mkrn*2 contributes to increased p53 and PERP levels, thereby facilitating aberrant p53/PERP-mediated apoptosis. Our findings strongly support the notion that the expression levels of *Mkrn*2 play a critical role in male germ cell development.
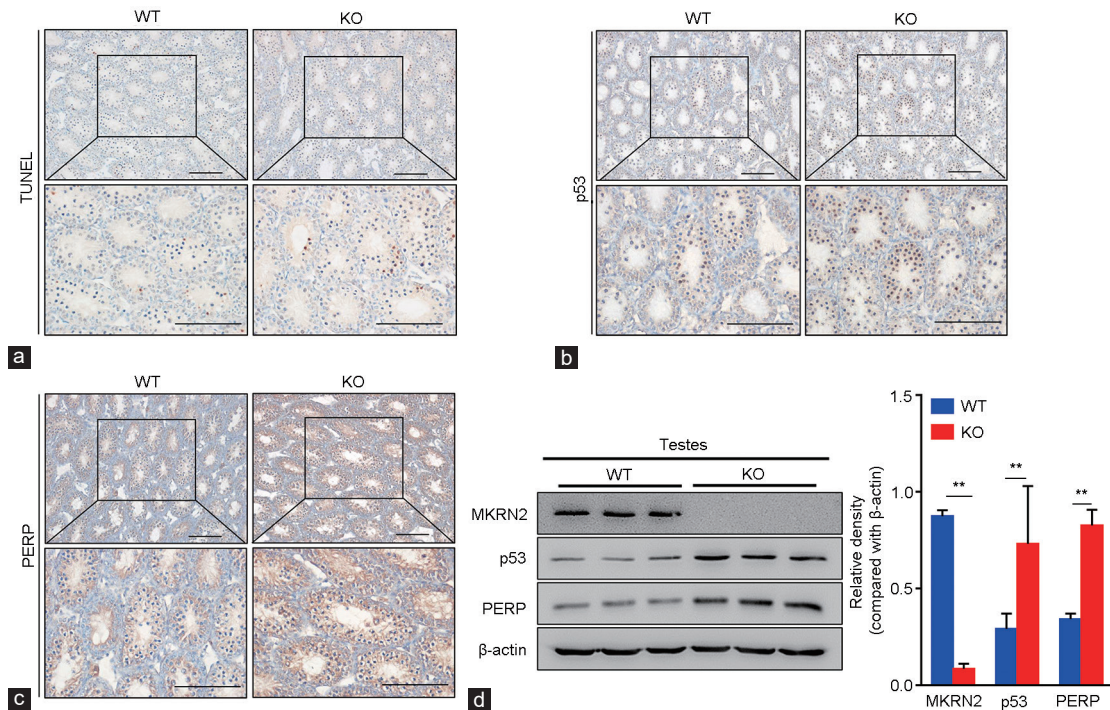
Figure 5: p53/PERP expression levels in *Mkrn2*-KO mouse testes. (**a**) TUNEL assay to assess the levels of apoptosis in *Mkrn2* KO versus WT mouse testis. Immunohistochemical staining of (**b**) p53 and (**c**) PERP expression in the testes of *Mkrn2*-KO and *Mkrn2*-WT mice. Scale bars=50 μm. (**d**) Western blot assay to test expression levels of MKRN2, p53, and PERP (left); and the different densitometric levels between two groups: *Mkrn2*-KO and *Mkrn2*-WT mouse testes are analyzed by the two-tailed, unpaired Student's *t*-test to compare the data of the two groups from three independent experiments (right). **Significant difference at $P < 0.01$. Mkrn2: makorin-2; KO: knockout; WT: wild type; PERP: p53 apoptosis effector related to PMP22; MEF: mouse embryonic fibroblast; TUNEL: terminal deoxynucleotidyl transferase dUTP nick end labeling.

AUTHOR CONTRIBUTIONS

YCQ and YXX performed experiments, analyzed data, and wrote the main manuscript text. CSW, ZMS, and CFJ maintained mice and acquired data. YYT performed IHC. XQ and LW performed cell culture experiments. BHJ designed and supervised the project and helped to prepare and revise the manuscript. All authors read and approved the final version of the manuscript.

COMPETING INTERESTS

All authors declare no competing interests.

ACKNOWLEDGMENTS

REFERENCES

1. Martincic DS, Virant Klun I, Zorn B, Vrtovec HM. Germ cell apoptosis in the human testis. *Pflugers Arch* 2001; 442: R159–60.
2. Russell LD, Chiarini-Garcia H, Korsmeyer SJ, Knudson CM. *Bax*-dependent spermatogonia apoptosis is required for testicular development and spermatogenesis. *Biol Reprod* 2002; 66: 950–8.
3. Shaha C, Tripathi R, Mishra DP. Male germ cell apoptosis: regulation and biology. *Philos Trans R Soc Lond B Biol Sci* 2010; 365: 1501–15.
4. Xu L, Lu Y, Han D, Yao R, Wang H, *et al. Rnf138* deficiency promotes apoptosis of spermatogonia in juvenile male mice. *Cell Death Dis* 2017; 8: e2795.
5. Zhao XF, Wang Q, Ji YL, Wang H, Liu P, *et al.* Fenvalerate induces germ cell apoptosis in mouse testes through the Fas/FasL signaling pathway. *Arch Toxicol* 2011; 85: 1101–8.
6. Solek P, Majchrowicz L, Bloniarz D, Krotoszynska E, Koziorowski M. Pulsed or continuous electromagnetic field induce p53/p21-mediated apoptotic signaling pathway in mouse spermatogenic cells *in vitro* and thus may affect male fertility. *Toxicology* 2017; 382: 84–92.
7. Napoletano F, Gibert B, Yacobi-Sharon K, Vincent S, Favrot C, *et al.* p53-dependent programmed necrosis controls germ cell homeostasis during spermatogenesis. *PLoS Genet* 2017; 13: e1007024.
8. Hou S, Xian L, Shi P, Li C, Lin Z, *et al.* The *Magea* gene cluster regulates male germ cell apoptosis without affecting the fertility in mice. *Sci Rep* 2016; 6: 26735.
9. Sharpe RM. Environmental/lifestyle effects on spermatogenesis. *Philos Trans R Soc Lond B Biol Sci* 2010; 365: 1697–712.
10. Chen Y, Wang J, Zhang Q, Xiang Z, Li D, *et al.* Microcystin-leucine arginine exhibits immunomodulatory roles in testicular cells resulting in orchitis. *Environ Pollut* 2017; 229: 964–75.
11. Puscheck E, Philip PA, Jeyendran RS. Male fertility preservation and cancer treatment. *Cancer Treat Rev* 2004; 30: 173–80.
12. Choy JT, Brannigan RE. The determination of reproductive safety in men during and after cancer treatment. *Fertil Steril* 2013; 100: 1187–91.
13. Omwancha J, Zhou XF, Chen SY, Baslan T, Fisher CJ, *et al.* Makorin RING finger protein 1 (MKRN1) has negative and positive effects on RNA polymerase II-dependent transcription. *Endocrine* 2006; 29: 363–73.
14. Zhang QH, Ye M, Wu XY, Ren SX, Zhao M, *et al.* Cloning and functional analysis of cDNAs with open reading frames for 300 previously undefined genes expressed in CD34+ hematopoietic stem/progenitor cells. *Genome Res* 2000; 10: 1546–60.
15. Gray TA, Azama K, Whitmore K, Min A, Abe S, *et al.* Phylogenetic conservation of the makorin-2 gene, encoding a multiple zinc-finger protein, antisense to the *RAF1* proto-oncogene. *Genomics* 2001; 77: 119–26.
16. Yang PH, Cheung WK, Peng Y, He ML, Wu GQ, *et al.* Makorin-2 is a neurogenesis inhibitor downstream of phosphatidylinositol 3-kinase/Akt (PI3K/Akt) signal. *J Biol Chem* 2008; 283: 8486–95.
17. Qian X, Wang L, Zheng B, Shi ZM, Ge X, *et al.* Deficiency of *Mkrn2* causes abnormal spermiogenesis and spermiation, and impairs male fertility. *Sci Rep* 2016; 6: 39318.
18. Beumer TL, Roepers-Gajadien HL, Gademan IS, van Buul PP, Gil-Gomez G, *et al.* The role of the tumor suppressor p53 in spermatogenesis. *Cell Death Differ* 1998; 5: 669–77.
19. Oldereid NB, Angelis PD, Wiger R, Clausen OP. Expression of Bcl-2 family proteins and spontaneous apoptosis in normal human testis. *Mol Hum Reprod* 2001; 7: 403–8.

20 Duan P, Hu C, Butler HJ, Quan C, Chen W, *et al*. 4-Nonylphenol induces disruption of spermatogenesis associated with oxidative stress-related apoptosis by targeting p53-Bcl-2/Bax-Fas/FasL signaling. *Environ Toxicol* 2017; 32: 739–53.

21 Gong ZK, Wang SJ, Huang YQ, Zhao RQ, Zhu QF, *et al*. Identification and validation of suitable reference genes for RT-qPCR analysis in mouse testis development. *Mol Genet Genomics* 2014; 289: 1157–69.

22 Rondanino C, Maouche A, Dumont L, Oblette A, Rives N. Establishment, maintenance and functional integrity of the blood-testis barrier in organotypic cultures of fresh and frozen/thawed prepubertal mouse testes. *Mol Hum Reprod* 2017; 23: 304–20.

23 Dumont L, Chalmel F, Oblette A, Berby B, Rives A, *et al*. Evaluation of apoptotic- and autophagic-related protein expressions before and after IVM of fresh, slow-frozen and vitrified pre-pubertal mouse testicular tissue. *Mol Hum Reprod* 2017; 23: 738–54.

24 Subramanian A, Tamayo P, Mootha VK, Mukherjee S, Ebert BL, *et al*. Gene set enrichment analysis: a knowledge-based approach for interpreting genome-wide expression profiles. *Proc Natl Acad Sci U S A* 2005; 102: 15545–50.

25 Mootha VK, Lindgren CM, Eriksson KF, Subramanian A, Sihag S, *et al*. PGC-1alpha-responsive genes involved in oxidative phosphorylation are coordinately downregulated in human diabetes. *Nat Genet* 2003; 34: 267–73.

26 Wang J, Tang C, Wang Q, Su J, Ni T, *et al*. NRF1 coordinates with DNA methylation to regulate spermatogenesis. *FASEB J* 2017; 31: 4959–70.

27 Gopinathan L, Szmyd R, Low D, Diril MK, Chang HY, *et al*. Emi2 is essential for mouse spermatogenesis. *Cell Rep* 2017; 20: 697–708.

28 Shin C, Ito Y, Ichikawa S, Tokunaga M, Sakata-Sogawa K, *et al*. MKRN2 is a novel ubiquitin E3 ligase for the p65 subunit of NF-kappaB and negatively regulates inflammatory responses. *Sci Rep* 2017; 7: 46097.

29 Lee KY, Chan KY, Tsang KS, Chen YC, Kung HF, *et al*. Ubiquitous expression of MAKORIN-2 in normal and malignant hematopoietic cells and its growth promoting activity. *PLoS One* 2014; 9: e92706.

30 Yan HH, Mruk DD, Lee WM, Cheng CY. Ectoplasmic specialization: a friend or a foe of spermatogenesis? *Bioessays* 2007; 29: 36–48.

31 Cheng CY, Mruk DD. A local autocrine axis in the testes that regulates spermatogenesis. *Nat Rev Endocrinol* 2010; 6: 380–95.

32 Lin WW, Lamb DJ, Wheeler TM, Abrams J, Lipshultz LI, *et al*. Apoptotic frequency is increased in spermatogenic maturation arrest and hypospermatogenic states. *J Urol* 1997; 158: 1791–3.

33 Streichemberger E, Perrin J, Saias-Magnan J, Karsenty G, Malzac P, *et al*. Case report of apoptosis in testis of four *AZFc*-deleted patients: increased DNA fragmentation during meiosis, but decreased apoptotic markers in post-meiotic germ cells. *Hum Reprod* 2012; 27: 1939–45.

34 Liu T, Wang L, Chen H, Huang Y, Yang P, *et al*. Molecular and cellular mechanisms of apoptosis during dissociated spermatogenesis. *Front Physiol* 2017; 8: 188.

35 Zheng S, Turner TT, Lysiak JJ. Caspase 2 activity contributes to the initial wave of germ cell apoptosis during the first round of spermatogenesis. *Biol Reprod* 2006; 74: 1026–33.

36 Jahnukainen K, Chrysis D, Hou M, Parvinen M, Eksborg S, *et al*. Increased apoptosis occurring during the first wave of spermatogenesis is stage-specific and primarily affects midpachytene spermatocytes in the rat testis. *Biol Reprod* 2004; 70: 290–6.

37 Correia S, Cardoso HJ, Cavaco JE, Socorro S. Oestrogens as apoptosis regulators in mammalian testis: angels or devils? *Expert Rev Mol Med* 2015; 17: e2.

38 Okamoto T, Coultas L, Metcalf D, van Delft MF, Glaser SP, *et al*. Enhanced stability of Mcl1, a prosurvival Bcl2 relative, blunts stress-induced apoptosis, causes male sterility, and promotes tumorigenesis. *Proc Natl Acad Sci U S A* 2014; 111: 261–6.

39 Arkoun B, Dumont L, Milazzo JP, Way A, Bironneau A, *et al*. Retinol improves *in vitro* differentiation of pre-pubertal mouse spermatogonial stem cells into sperm during the first wave of spermatogenesis. *PLoS One* 2015; 10: e0116660.

40 Baumer N, Sandstede ML, Diederichs S, Kohler G, Readhead C, *et al*. Analysis of the genetic interactions between cyclin A1, Atm and p53 during spermatogenesis. *Asian J Androl* 2007; 9: 739–50.

41 Awais R, Spiller DG, White MR, Paraoan L. p63 is required beside p53 for PERP-mediated apoptosis in uveal melanoma. *Br J Cancer* 2016; 115: 983–92.

42 Kiseljak-Vassiliades K, Mills TS, Zhang Y, Xu M, Lillehei KO, *et al*. Elucidating the role of the desmosome protein p53 apoptosis effector related to PMP-22 (PERP) in growth hormone tumors. *Endocrinology* 2017; 158: 1450–60.

43 Paraoan L, Gray D, Hiscott P, Ebrahimi B, Damato B, *et al*. Expression of p53-induced apoptosis effector PERP in primary uveal melanomas: downregulation is associated with aggressive type. *Exp Eye Res* 2006; 83: 911–9.

44 Davies L, Spiller D, White MR, Grierson I, Paraoan L. PERP expression stabilizes active p53 via modulation of p53-MDM2 interaction in uveal melanoma cells. *Cell Death Dis* 2011; 2: e136.

45 Vera M, Biswas J, Senecal A, Singer RH, Park HY. Single-cell and single-molecule analysis of gene expression regulation. *Annu Rev Genet* 2016; 50: 267–91.

46 Hafner A, Bulyk ML, Jambhekar A, Lahav G. The multiple mechanisms that regulate p53 activity and cell fate. *Nat Rev Mol Cell Biol* 2019; 20: 199–210.

47 Tang Y, Zhao W, Chen Y, Zhao Y, Gu W. Acetylation is indispensable for p53 activation. *Cell* 2008; 133: 612–26.

48 Sykes SM, Mellert HS, Holbert MA, Li K, Marmorstein R, *et al*. Acetylation of the p53 DNA-binding domain regulates apoptosis induction. *Mol Cell* 2006; 24: 841–51.

49 Tang Y, Luo J, Zhang W, Gu W. Tip60-dependent acetylation of p53 modulates the decision between cell-cycle arrest and apoptosis. *Mol Cell* 2006; 24: 827–39.
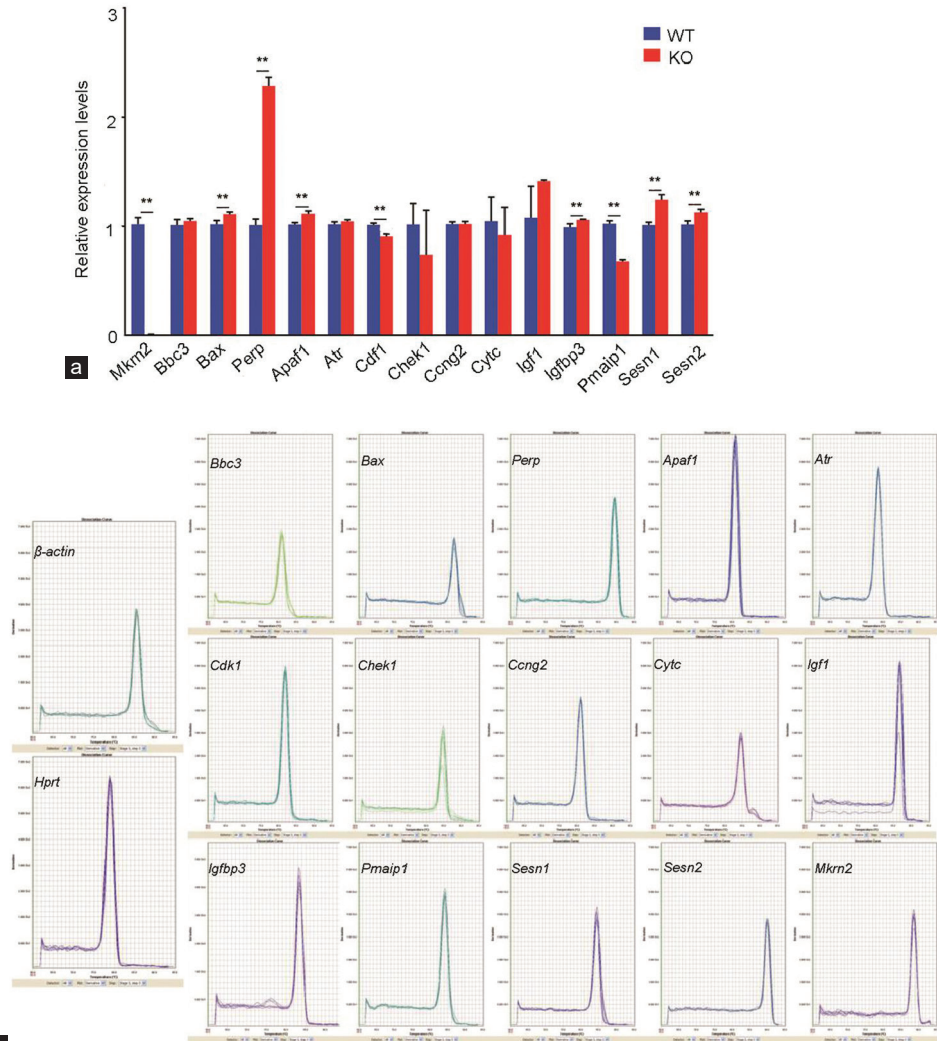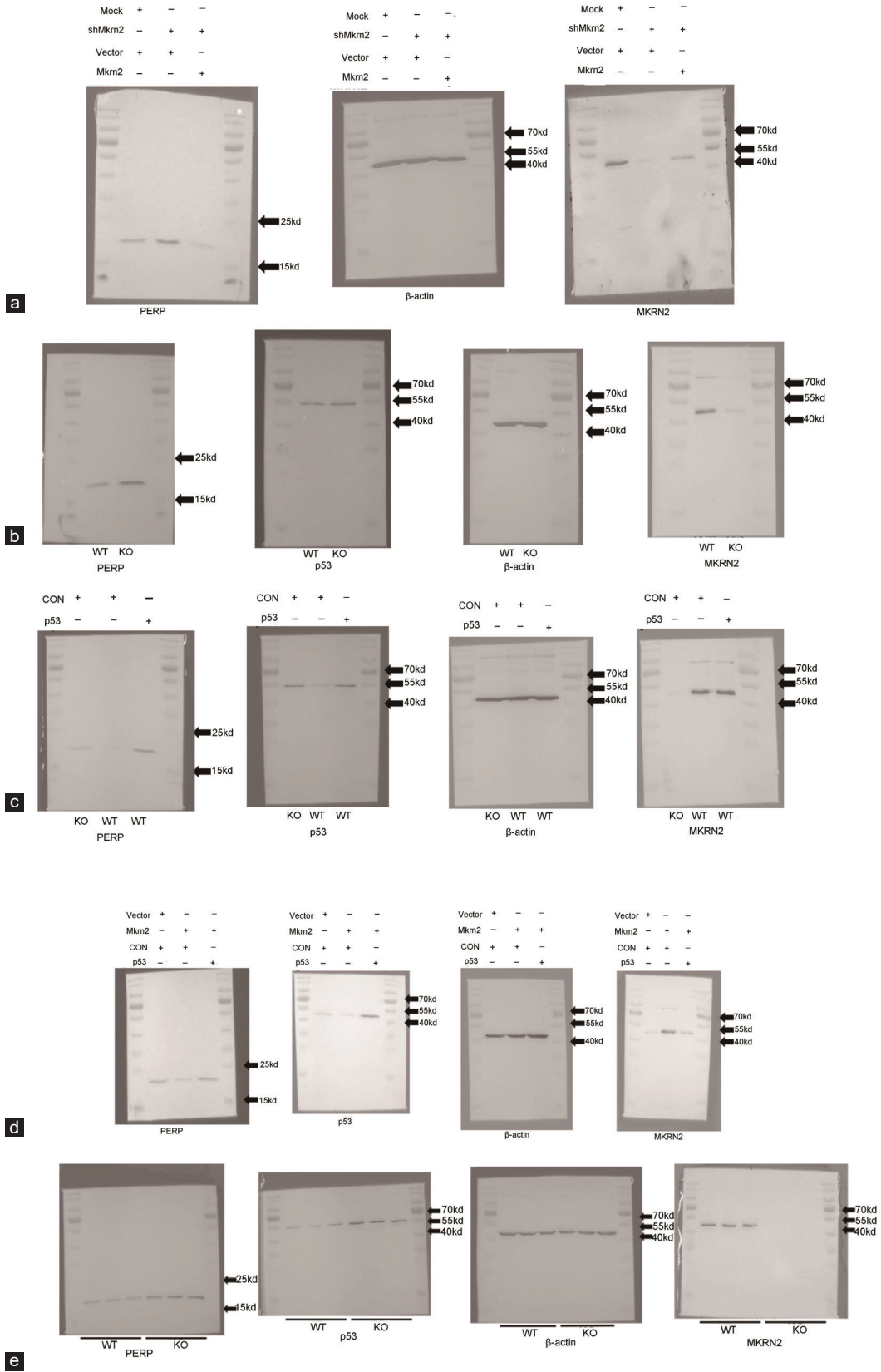
Supplementary Figure 1: *Mkrn*2 affects the expression levels of *Perp* mRNA. (**a**) The expression levels of DEGs between *Mkrn*2 WT vs. KO MEFs are analyzed by qRT-PCR, and (**b**) the corresponding melting curve are acquired from the 7900HT system. Data are represented as the means ± SD and analyzed by the two-tailed, unpaired Student's *t*-test. ** $P<0.01$

Supplementary Figure 2: The originals of Western blots
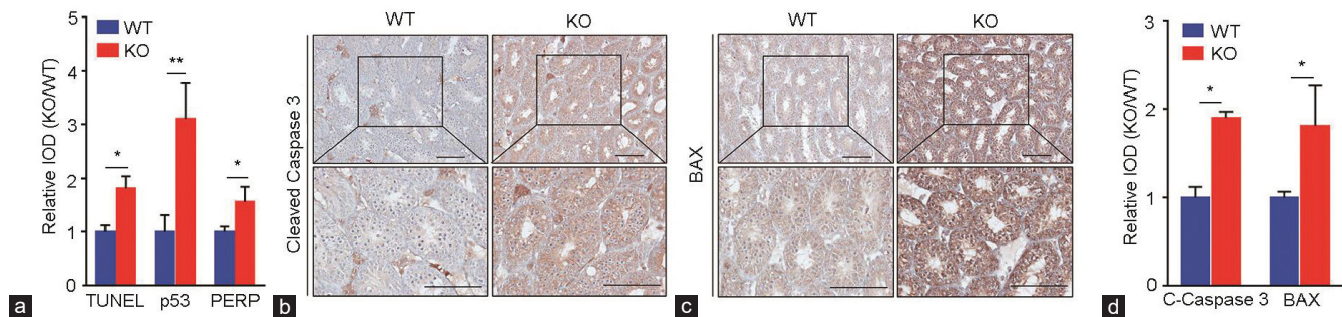
Supplementary Figure 3: *Mkrn*2 KO and the apoptosis levels of testes. (**a**) The relative IOD of TUNEL, p53 and PERP are calculated by Image-Pro Plus software. (**b, c**) Immunohistochemical staining of Cleaved Caspase 3 (C-Caspase 3) and BAX in testes of *Mkrn2* KO and WT mice. Scale bar: 50 μm. (**d**) The relative IOD values of C-Caspase 3 and BAX are analyzed by Image-Pro Plus software. Data are represented and analyzed by the two-tailed, unpaired Student's *t*-test from three independent experiments and each performed for three times. *$P<0.05$, **$P<0.01$
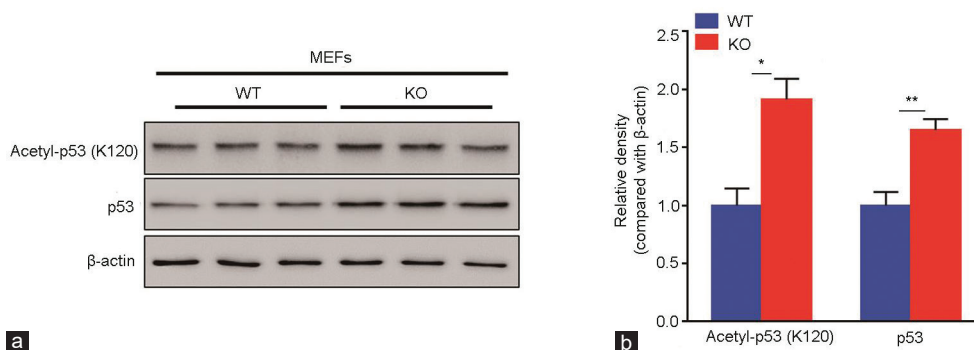
Supplementary Figure 4: *Mkrn*2 KO increases the acetylation levels of p53 (K120) in MEFs. (**a**) Western blotting is used to determine protein levels of p53 and acetylated-p53 (K120) in WT and KO MEFs, and (b) the relative density levels are quantified by Image J software. Data are presented and analyzed by the two-tailed, unpaired Student's t-test from experiments performed in triplicate. * $P<0.05$, ** $P<0.01$.

Supplementary Table 1: The generation of *Mkrn2* KO and WT Mice

Male (n)	Female (n)	Number	Pups	Genotype/gender (n)
+/- (2)	+/- (4)	6	♂13 ♀3	+/+♂6
				+/-♂5♀2
				-/-♂2♀1
+/- (2)	-/- (4)	6	♂9 ♀6	+/-♂5♀4
				-/-♂4♀2

+/+: *Mkrn2* WT +/-: *Mkrn2* heterozygous -/-: *Mkrn2* KO

Supplementary Table 2: Primers used in this study

Primer name	Sequence 5'-3'
qRT-PCR	
β-actin-F	GGCTGTATTCCCCTCCATCG
β-actin-R	CCAGTTGGTAACAATGCCATGT
Hprt-F	TCAGTCAACGGGGGACATAAA
Hprt-R	GGGGCTGTACTGCTTAACCAG
Mkrn2-F	GTCCTGCACCCAACCCTTC
Mkrn2-R	CACCAGCGTCTTCTTCTCCC
Bbc3-F	AGCAGCACTTAGAGTCGCC
Bbc3-R	CCTGGGTAAGGGGAGGAGT
Bax-F	TGAAGACAGGGGCCTTTTTG
Bax-R	AATTCGCCGGAGACACTCG
Perp-F	ATCGCCTTCGACATCATCGC
Perp-R	CCCCATGCGTACTCCATGAG
Apaf1-F	AGTAATGGGTCCTAAGCATGTTG
Apaf1-R	GCGATTGGGAAAATCACGTAAAA
Atr-F	GAATGGGTGAACAATACTGCTGG
Atr-R	TTTGGTAGCATACACTGGCGA
Cdk1-F	AGAAGGTACTTACGGTGTGGT
Cdk1-R	GAGAGATTTCCCGAATTGCAGT
Chek1-F	CTTGGTCAAAAGAATGACGAGGT
Chek1-R	CCGTCGCCTTTAGAAAGTCGG
Ccng2-F	AGGGGTTCAGCTTTTCGGATT
Ccng2-R	AGTGTTATCATTCTCCGGGGTAG
Cyct-F	GGTGGAAAAAGGCGGGAAAC
Cyct-R	CCGTGTAAGAAAATCCTGGTGC
Igf1-F	CTGGACCAGAGACCCTTTGC
Igf1-R	GGACGGGGACTTCTGAGTCTT
Igfbp3-F	CACACCGAGTGACCGATTCC
Igfbp3-R	GTGTCTGTGCTTTGAGACTCAT
Pmaip1-F	GCAGAGCTACCACCTGAGTTC
Pmaip1-R	CTTTTGCGACTTCCCAGGCA
Sesn1-F	GGCCAGGACGAGGAACTTG
Sesn1-R	AAGGAGTCTGCAAATAACGCAT
Sesn2-F	TCCGAGTGCCATTCCGAGAT
Sesn2-R	TCCGGGTGTAGACCCATCAC
Gapdh-F	AGGTCGGTGTGAACGGATTTG
Gapdh-R	TGTAGACCATGTAGTTGAGGTCA

F: Forward, R: Reverse